Single-Molecule Dynamics of the Calcium-Dependent Activation of Plasma-Membrane Ca^{2+}-ATPase by Calmodulin

Kenneth D. Osborn,* Asma Zaidi,† Abhijit Mandal,* Ramona J. Bieber Urbauer,‡ and Carey K. Johnson*

*Department of Chemistry, †Department of Pharmacology and Toxicology, and ‡Department of Molecular Biology, University of Kansas, Lawrence, Kansas

ABSTRACT The plasma membrane calcium-ATPase (PMCA) helps to control cytosolic calcium levels by pumping out excess Ca^{2+}. PMCA is regulated by the Ca^{2+} signaling protein calmodulin (CaM), which stimulates PMCA activity by binding to an autoinhibitory domain of PMCA. We used single-molecule polarization methods to investigate the mechanism of regulation of the PMCA by CaM fluorescently labeled with tetramethylrhodamine. The orientational mobility of PMCA-CaM complexes was determined from the extent of modulation of single-molecule fluorescence upon excitation with a rotating polarization. At a high Ca^{2+} concentration, the distribution of modulation depths reveals that CaM bound to PMCA is orientationally mobile, as expected for a dissociated autoinhibitory domain of PMCA. In contrast, at a reduced Ca^{2+} concentration a population of PMCA-CaM complexes appears with significantly reduced orientational mobility. This population can be attributed to PMCA-CaM complexes in which the autoinhibitory domain is not dissociated, and thus the PMCA is inactive. The presence of these complexes demonstrates the inadequacy of a two-state model of Ca^{2+} pump activation and suggests a regulatory role for the low-mobility state of the complex. When ATP is present, only the high-mobility state is detected, revealing an altered interaction between the autoinhibitory and nucleotide-binding domains.

INTRODUCTION

The Ca^{2+}-binding protein calmodulin (CaM, molecular weight 16.7 kDa) binds and activates target proteins in response to a Ca^{2+} signal (Crivici and Ikura, 1995; Vogel, 1994; Van Eldik and Watterson, 1998). CaM is thus linked to numerous intracellular regulatory pathways. CaM consists of two globular domains connected by a central helix (Babu et al., 1988). Upon binding of Ca^{2+}, CaM undergoes conformational changes that facilitate binding and activation of a wide variety of target proteins having little sequence homology (Crivici and Ikura, 1995).

One of the best characterized targets of CaM is the plasma-membrane Ca^{2+}-ATPase (PMCA), a Ca^{2+} pump that functions to maintain the low intracellular Ca^{2+} levels necessary for Ca^{2+} signaling (Carafoli, 1987; Penniston and Enyedi, 1998). The PMCA is a 134-kDa protein with 10 transmembrane segments. A large intracellular loop located between transmembrane segments 4 and 5 contains the ATP-binding site and a phosphorylatable aspartate residue. The CaM-binding domain is located near the C-terminus of PMCA. This site has been suggested to function as an autoinhibitory domain that regulates activity of the pump by binding to the cytosolic loops between transmembrane segments 2 and 3 and between transmembrane segments 4 and 5, thereby blocking ATP binding or utilization (Enyedi et al., 1989). CaM binding leads to dissociation of this domain, allowing utilization of ATP and thus activating the enzyme. Although the concept that CaM activates PMCA by removing the autoinhibitory domain from the active site is widely accepted, the dynamic interactions between CaM and the inhibitory region of the PMCA have not been well characterized, particularly with regard to the roles of Ca^{2+} and ATP.

In contrast to ensemble methods, in which detailed information about individual members of a heterogeneous system is lost due to averaging over the ensemble, single-molecule spectroscopy has emerged as a powerful tool to characterize the distribution of properties in a heterogeneous population of molecules (Noji et al., 1997; Xie and Trautman, 1998; Lu et al., 1998; Moerner and Orrit, 1999; Weiss, 1999; Xie and Lu, 1999). The polarization of the light used to excite a single molecule provides a means to probe the orientational dynamics of single molecules (Xie and Dunn, 1994; Ha et al., 1999; Warshaw et al., 1998; Adachi et al., 2000; Sosa et al., 2001; Forkey et al., 2003). In this study, the polarization of the excitation beam was rotated continuously and the fluorescence intensity from single molecules recorded. The extent to which the fluorescence intensity is modulated by the polarization of the excitation beam is a measure of the mobility of the fluorophore (Ha et al., 1999). A fluorophore with fixed orientation experiences maximum excitation when the orientation of the polarization aligns with the transition dipole of the dye and minimum excitation when the polarization is orthogonal to the transition dipole of the dye molecule. As a result, the fluorescence signal from an orientationally immobile single molecule is modulated. On the other hand, if the transition dipole reorients rapidly on the timescale of the polarization

Submitted December 30, 2003, and accepted for publication May 17, 2004.

Address reprint requests to Carey K. Johnson, Dept. of Chemistry, University of Kansas, 1251 Wescoe Hall Dr., Lawrence, KS 66045. E-mail: ckjohnson@ku.edu.

Ramona J. Bieber Urbauer's present address is Dept. of Biochemistry and Molecular Biology, University of Georgia, Athens, GA 30602.

0006-3495/04/09/1892/08 $2.00

doi: 10.1529/biophysj.103.039404

modulation, the modulation of the fluorescence signal is reduced or eliminated.

We have detected Ca^{2+}-dependent binding of CaM to single PMCA molecules and have investigated the dynamics of calmodulin (CaM) bound to PMCA. By application of single-molecule polarization modulation techniques it has been possible to characterize dynamic structures of PMCA-CaM complexes that would otherwise be hidden in the ensemble average. The experiments described here probed the mobility of CaM labeled with a tetramethylrhodamine-5-maleimide (TMR) fluorophore and bound to PMCA. The results reveal two populations of PMCA-CaM complexes having distinct orientational mobilities. The orientational mobility distributions depend on the Ca^{2+} level and the presence or absence of ATP. We find that the mobility of the CaM-binding domain of PMCA correlates with regulation of the activity of the enzyme. The orientational mobilities are not consistent with a two-state model (Enyedi et al., 1989; Falchetto et al., 1991), which dictates that when CaM is bound to PMCA the autoinhibitory domain is dissociated from the nucleotide-binding region of the pump. Our results suggest an intermediate state in the activation of the pump, in which CaM is bound (or perhaps partially bound by one of its two globular domains) but the autoinhibitory domain is still associated with the active site.

METHODS

Materials

The detergent $C_{12}E_8$ was obtained from Calbiochem (La Jolla, CA). CaM-sepharose was a product of Pharmacia Biotech (Piscataway, NJ). ATP, adenosine 5′-(β,γ-imido)triphosphate (AMP-PNP), and phosphatidylcholine were purchased from Sigma Chemical Company (St. Louis, MO). All other reagents were of the highest purity grade available.

Fluorescence labeling

Calmodulin was modified by site-directed mutagenesis to replace the threonine residue at position 34 with a cysteine as described previously (Allen et al., 2004). The residue was fluorescently labeled with TMR (Molecular Probes, Eugene, OR) following standard protocols provided by the supplier. A 10-fold excess of tris-(2-carboxyethyl)phosphine hydrochloride was added to CaM-T34C (50–100 mM) to reduce any disulfide bonds. TMR was then added in a 10-fold excess and the solution was shaken mildly for ~1 h. The labeled protein was purified by repeated dialysis followed by high-performance liquid chromatography (HPLC) separation. The labeling efficiency was found to be >90% as determined by HPLC purification and verification by mass spectrometry.

Purification of PMCA

PMCA was purified from freshly drawn human blood by affinity chromatography using CaM-sepharose as described elsewhere (Niggli et al., 1981). Membranes were solubilized with Triton X-100 (1 mg/mg protein) and stabilized with phosphatidylcholine and Ca^{2+} (final concentrations of 0.5 mg/ml and 100 μM, respectively). To elute the solubilized PMCA from the CaM-sepharose column, ethylene diamine tetraacetic acid (EDTA) was used to sequester free Ca^{2+}, resulting in loss of the affinity of CaM for PMCA. Active fractions were pooled and $MgCl_2$ and $CaCl_2$ added to neutralize the EDTA. The enzyme was stored at −80°C with no loss of activity.

Measurement of PMCA activity

The activity of PMCA was determined in 96-well microplates containing 25 mM Tris-HCl, pH 7.4, 50 mM KCl, 1 mM $MgCl_2$, 0.1 mM ouabain, 4 μg/ml oligomycin, 200 μM ethylene glycol-bis(2-aminoethylether)-N,N,N′,N′-tetraacetic acid (EGTA), and enough $CaCl_2$ added to yield the desired final free Ca^{2+} concentration in a volume of 100 μl. The final free Ca^{2+} concentration was calculated using a modified version of a computer program that calculates the multiple equilibria between all ligands in solution (Fabiato and Fabiato, 1979). The PMCA activity measured in the presence of Ca^{2+} but with no CaM is referred to as ''basal'' activity and that in the presence of Ca^{2+} and 120 nM CaM as ''CaM-stimulated activity.'' After a 5-min preincubation of PMCA with other components of the assay, the reaction was started by the addition of 1 mM ATP, continued for 20 min at 37°C, and stopped by the addition of Malachite Green dye solution (Lanzetta et al., 1979). The contents were made acidic by addition of 19.5% H_2SO_4, incubated for 45 min, and the absorbance read at 650 nm in a microwell plate reader. The PMCA activity was defined as the Ca^{2+}-activated ATP hydrolysis and expressed as nanomoles of inorganic phosphate liberated per mg protein per min, based on values from a standard curve of the absorbance using various concentrations of free inorganic phosphate.

Sample conditions

Buffer conditions for the saturating Ca^{2+} experiments were 10 mM HEPES (pH 7.4), 0.1 M KCl, 1 mM $MgCl_2$, and 100 μM $CaCl_2$. The final free Ca^{2+} concentration was 25 μM after accounting for the amount of Ca^{2+} and EDTA added in the PMCA storage buffer. Experiments done at 0.15 μM free Ca^{2+} used the same buffer conditions with the addition of 10 mM EGTA and sufficient $CaCl_2$ and $MgCl_2$ to buffer Ca^{2+} at the desired ion concentrations. A third buffer identical in pH and in KCl and HEPES concentrations but lacking $CaCl_2$ or $MgCl_2$ provided a final free Ca^{2+} concentration of 2 nM with the addition of 1 mM EGTA to bind the minimal free Ca^{2+} introduced from the PMCA storage solution. A concentration of 1 mM ATP or AMP-PNP was used for experiments done in the presence of nucleotide.

Binding of CaM-TMR to PMCA was carried out in the dark at 4°C for at least 30 min or at room temperature for 15 min. For samples containing ATP, the nucleotide was added immediately after the binding of CaM to PMCA and prior to mixing with the agarose gel (Sigma, Type VIIA). Samples were mixed with agarose gel held slightly above the gelling temperature to yield a final gel concentration of 2.2%. PMCA and CaM-TMR were added to yield concentrations of 7.5 nM and 0.35 nM, respectively. This mixture was placed on a clean, dry coverslip held over a cold block to facilitate rapid setting of the gel. Once the gel was set, a clean coverslip was placed on top of the gel to minimize drying of the sample during the experiments.

Single-molecule spectroscopy

The samples were excited with a focused intensity of ~1 kW/cm^2 from a linearly polarized 542.5 nm HeNe laser (Research Electro-optics, Boulder, CO). The orientation of the polarization was continuously rotated by an electrooptic modulator (M-350, Conoptics, Danbury, CT) driven by a function generator (DS340, Stanford Research Systems, Sunnyvale, CA) at a frequency of 25 Hz followed by a quarter-wave plate. The excitation beam was passed through a filter (D543/10×, Chroma, McHenry, IL) and into the epi-illumination port of the microscope where it was reflected by

a dichroic mirror (Q555LP, Chroma) onto a 100×, 1.3 numerical aperture objective lens (Nikon Superfluor, Melville, NY). Fluorescence was collected by the objective lens, transmitted through the dichroic mirror and an emission filter (HQ600/80m, Chroma), and focused onto an avalanche photodiode (SPCM-AQR-14, Perkin-Elmer Optoelectronics, Vaudreuil, Quebec, Canada). Signals from the photodiodes were processed by a PCI-6052E card (National Instruments, Austin, TX) for images. This card was also used for control of the closed-loop nanopositioning scanning stage (Nano-H100, Mad City Labs, Madison, WI). A PCI-6602 PC plug-in card (National Instruments) was used to collect fluorescence trajectories with 2 ms per channel bin width. Analysis of the data was performed by in-house software using a maximum-likelihood estimator (MLE)-based fitting algorithm described previously (Osborn et al., 2003). The bulk fluorescence anisotropy decay measurement on CaM-TMR was carried out with a time-domain fluorescence lifetime instrument described elsewhere (Harms et al., 1997) with excitation pulses at 560 nm.

RESULTS

Activity of PMCA-CaM-TMR

PMCA exists as four different isoforms, though not all tissues express the four gene products. Red blood cell membranes are highly enriched in isoform 4, known to be ubiquitously present in almost all tissues and thought to perform a housekeeping function in intracellular Ca^{2+} regulation (Stauffer et al., 1995). The activity of purified PMCA was measured over a range of Ca^{2+} concentrations. In the absence of CaM, basal activity of PMCA increased with increasing Ca^{2+}, leveling off at a V_{max} of 280 nmoles P_i/mg/min in the 100–500 μM Ca^{2+} range, consistent with earlier reports (Niggli et al., 1981). Addition of CaM-TMR at a saturating concentration (120 nM) resulted in significant activation of Ca^{2+}-dependent ATPase activity with an increase in the V_{max} of PMCA to 675 nmoles P_i /mg/min. This was accompanied by a decline in K_{act} of PMCA for Ca^{2+} from 17 μM to 0.1 μM, indicating an increased affinity for Ca^{2+} in the presence of CaM-TMR. An essentially similar level of activation was observed with commercial CaM purified from bovine brain, demonstrating that fluorescent labeling of CaM results in no loss of efficacy in CaM for stimulation of PMCA activity, thus confirming the biological significance of our spectroscopic results.

Detection of PMCA-CaM binding

The purified PMCA was translationally restricted in an agarose gel (2.2%) to provide an aqueous environment for the sample. Fluorescence signals from immobilized single CaM-TMR molecules were observed only in the presence of both Ca^{2+} and PMCA. We have previously found that fluorescently labeled CaM is not immobilized in an agarose gel (Allen et al., 2004). We verified that single-molecule images were not detected for CaM-TMR in the absence of PMCA, nor were images detected in the presence of PMCA but without CaM-TMR. The signals can further be identified as coming from single molecules based on the low spot density of fluorescence images and by one-step photobleaching. Reduction of the Ca^{2+} concentration from a saturating level of 25 μM to 0.15 μM resulted in a density of single-molecule images of PMCA-CaM complexes within the scanned region (10 × 10 μm) of about one-half of the density at a saturating Ca^{2+} concentration, consistent with the reported $[Ca^{2+}]_{1/2}$ values of 0.2–1 μM for activation of PMCA by native CaM (Niggli et al., 1981). The presence of single-molecule images thus demonstrates specific binding of single CaM-TMR molecules to PMCA. Single-molecule images were absent in samples with PMCA and CaM-TMR at Ca^{2+} concentrations in the range of 2 nM. Thus, Ca^{2+}-free CaM does not bind to PMCA in our samples, in agreement with previous studies of PMCA-CaM binding (Enyedi et al., 1989). These observations demonstrate that the immobilization of CaM-TMR occurs through a Ca^{2+}-activated interaction with PMCA.

Single-molecule PMCA-CaM binding has been observed up to 2 h after formation of the gel, showing that binding of CaM to PMCA persists for long periods under conditions in which the CaM concentration ($\sim 6 \times 10^{-11}$ M) is well below the nominal dissociation constant for PMCA-CaM of 8 nM (Caride et al., 1999). This result is consistent with previous reports that the dissociation rate of CaM from PMCA isoform 4 is slow (0.03 min^{-1}) (Caride et al., 1999).

Polarization modulation trajectories

Polarization modulation measurements were carried out at Ca^{2+} concentrations of 25 μM, which is sufficient for maximum activation of PMCA, and 0.15 μM, which corresponds to roughly one-third of the maximal activation for PMCA-CaM complexes (Niggli et al., 1981). For studies at both saturating and low Ca^{2+} in the absence of ATP, 124 single-molecule trajectories were collected for analysis. With the addition of ATP, 208 and 230 trajectories were collected for saturating and low Ca^{2+} concentrations, respectively. Similarly, 117 and 112 trajectories were recorded for saturating and low-Ca^{2+} concentrations, respectively, in the presence of AMP-PNP, a nonhydrolyzable ATP analog. The data were fit period-by-period by an MLE method (Osborn et al., 2003) to determine values of the modulation depth. Regions with obvious dark states were avoided as described previously (Osborn et al., 2003). The average survival time of a molecule in this study was 11 s. Trajectories lasting 80 ms (two periods of modulation) or less were disregarded for fitting purposes.

Fig. 1 *A* shows a typical modulated trajectory for CaM bound to PMCA. An expanded region of the data is shown in the inset with the associated MLE-based fit. The average signal-to-background ratio in this experiment was 4:1, and any trajectory with less than a 3:1 signal-to-background was discarded. Both unmodulated background counts and projection of polarization onto the *z* axis in the focal region by the high numerical aperture objective (Ha et al., 1999) lead to a decrease in the maximum measured modulation depth. The

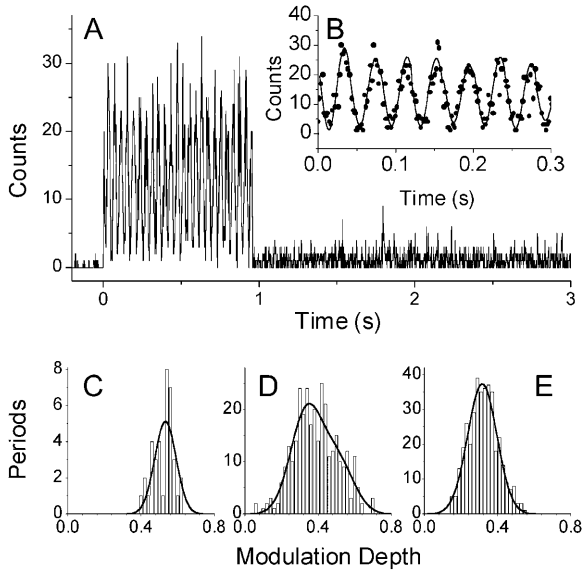

FIGURE 1 A typical polarization modulation trajectory of a single molecule of CaM-TMR bound to PMCA immobilized in an agarose gel (*A*). TMR was excited at 542 nm with polarization modulated at a rate of 25 Hz. An expanded region of this trajectory is shown in the inset (*B*) with the associated MLE-based fit. Modulation depth histograms of individual molecules that show high (*C*), intermediate (*D*), and low (*E*) modulation-depth distributions. The lines show fits of the distributions to single (*C* and *E*) or double (*D*) Gaussian functions with modulation depth distributions centered at 0.53 (*C*), 0.33 and 0.51 (*D*), and 0.32 (*E*).

average modulation depth expected for immobile molecules after accounting for these contributions is ~0.6. Variations in the signal-to-background level and a distribution of z components of the transition dipole contribute to the observed widths of the modulation depth distributions. These issues have been addressed in greater detail elsewhere (Osborn et al., 2003).

To investigate the extent of motion of the dye with respect to the protein, we measured the bulk fluorescence anisotropy decay of CaM-TMR and found rotational correlation times of 0.67 ± 0.13 ns and 10.6 ± 1.6 ns. (These results are included in the supplemental material.) The longer rotational correlation time, which represents two-thirds of the anisotropy decay amplitude, can be assigned to rotational motion of CaM-TMR as a whole, showing that TMR is to a large extent fixed to CaM with little independent motion of the dye. This finding is consistent with previous studies in which TMR attached to a protein via a single covalent bond nonetheless reports orientational motions of the protein to which it is attached (Warshaw et al., 1998; Peterman et al., 2001) and suggests that the attached TMR adheres non-covalently to the surface of the protein.

Distributions of modulation depths

Histograms were constructed of the modulation depths of each period of single-molecule trajectories. Fig. 1, *C* and *E*, shows examples of modulation-depth distributions and associated Gaussian fits for two molecules with average modulation depths of 0.53 and 0.32, respectively. The peak modulation depth in Fig. 1 *C* is close to that predicted for an orientationally immobile molecule considering the demodulating factors mentioned above, whereas the modulation depth in Fig. 1 *E* is significantly lower than could be explained by such factors. For most single-molecule polarization modulation trajectories, the modulation distributions fit well to a Gaussian distribution. We have observed previously that modulation-depth histograms for molecules with static orientational mobility can be fit well by a Gaussian function (Osborn et al., 2003), as would be expected for a single population distributed about a mean value with a width resulting from several sources including counting statistics and fluctuations in background. The observation of distributions that are approximately normally distributed suggests that the modulation depths reflect fluctuations within a single population. Thus, the single-molecule modulation depths appear in most cases to reflect distributions that are static on the timescale of the recorded fluorescence trajectories. In ~30% of the molecules, however, a broader distribution was observed, indicating that these molecules explored a wider range of mobilities. An example is shown in the distribution of modulation depths in Fig. 1 *D*. This distribution was fit to a double Gaussian distribution, with peaks centered at modulation depths of 0.33 and 0.51. This range of modulation depths cannot be attributed to variations in the signal-to-background over the course of the trajectory.

Because the majority of PMCA-CaM complexes displayed approximately Gaussian distributions of the modulation depth, we characterized each molecule by the average depth of modulation over its trajectory. Fig. 2 shows the distribution of modulation depths for single molecules at saturating (25 μM) and low (0.15 μM) Ca^{2+} concentrations. At a saturating Ca^{2+} concentration this distribution is narrow with a peak near 0.38. A tail in each distribution extends toward values of higher modulation depth. At 0.15 μM Ca^{2+}, the distribution of modulation depths displays a component that peaked at a modulation depth of 0.39 and a second population distribution centered at 0.61. To verify the reproducibility of this result, we have observed a population with an increased modulation depth at a subsaturating Ca^{2+} concentration of 0.15 μM with two different preparations of PMCA (Osborn, 2003).

Calcium transport by PMCA is coupled to binding and hydrolysis of ATP. Fig. 3 shows the average modulation depth for over 200 molcules at both 25-μM and 0.15-μM Ca^{2+} concentrations in the presence of ATP. At the higher calcium concentration, the distribution is similar to the distribution in the absence of ATP (Fig. 2), with an average modulation depth of 0.40. In contrast to the effect of Ca^{2+} in the absence of ATP, the modulation-depth distribution obtained with ATP at 0.15 μM Ca^{2+} is effectively unchanged (average 0.39) from the distribution at 25 μM

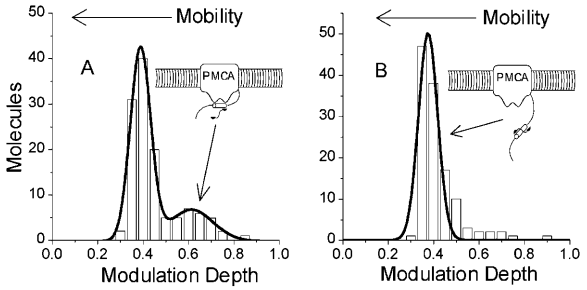

FIGURE 2 Single-molecule modulation-depth histograms for CaM-TMR bound to fresch PMCA at a Ca^{2+} concentration of 0.15 μM (*A*), and a saturating Ca^{2+} concentration of 25 μM (*B*). Modulation depths were measured for a total of 124 molecules in each case. The lines show a fit to two Gaussians with peaks at modulation depths of 0.39 and 0.61 (*A*), and a single Gaussian fit with a peak at a modulation depth of 0.38 (*B*). The schematic in each panel illustrates the interpretation of modulation-depth distributions in terms of the mobility of a dissociated autoinhibitory domain (high-mobility, low modulation-depth distribution) or associated autoinhibitory domain (low-mobility, high modulation-depth distribution).

Ca^{2+}. The high-modulation (low-mobility) population that is present at 0.15 μM Ca^{2+} in the absence of ATP is suppressed by the addition of ATP.

Modulation-depth distributions were also measured for PMCA in the presence of the nonhydrolyzable ATP analog AMP-PNP. The results are also shown in Fig. 3. Again, the distribution at 25 μM Ca^{2+} is similar (average modulation depth 0.39) to the distribution measured in the absence of ATP. However, the distribution at 0.15 μM Ca^{2+} with AMP-PNP reveals the presence of a population with high modulation depth that more closely resembles the distribution in the absence of ATP (Fig. 2) than the distribution in the presence of ATP. Thus, in contrast to ATP, the nonhydrolyzable ATP analog, AMP-PNP, does not suppress the high modulation depth (low-mobility) population. The observation of a significant change in the modulation-depth distribution upon changes in biologically relevant parameters supports the interpretation of the changes in terms of properties of PMCA-CaM complexes. In particular, the altered distribution in the presence of AMP-PNP compared to ATP (nucleotides that differ in only one atom) would appear to support the biological significance of the results.

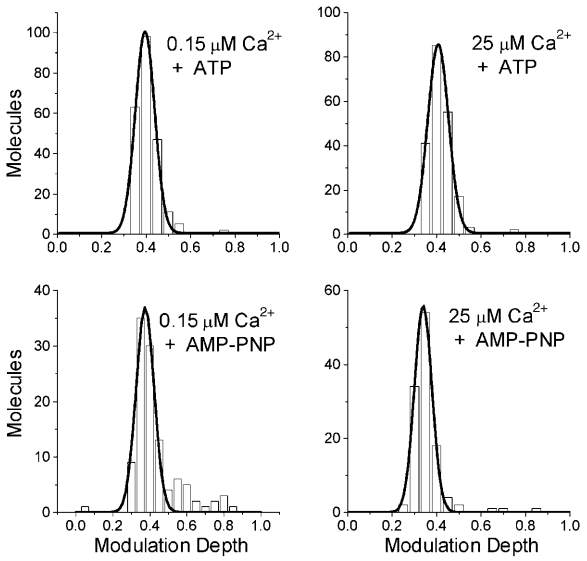

FIGURE 3 Histograms of single-molecule modulation depth histograms for CaM-TMR bound to fresh PMCA in the presence of ATP (*top panels*) and the nonhydrolyzable nucleotide analog AMP-PNP (*bottom panels*) at Ca^{2+} concentrations of 0.15 μM and 25 μM. Modulation depths were measured for a total of 208 molecules (25 μM Ca^{2+} with ATP), 230 molecules (0.15 μM Ca^{2+} with ATP), 117 molecules (25 μM Ca^{2+} with AMP-PNP), and 112 molecules (0.15 μM Ca^{2+} with AMP-PNP).

DISCUSSION

Orientational mobility of PMCA-CaM complexes

We have investigated the orientational mobility of single CaM-TMR molecules bound to translationally restricted PMCA by modulation of the polarization of the exciting light. The depth of modulation of the fluorescence intensity as the excitation polarization is rotated provides a measure of the orientational freedom of the fluorophore. Fig. 2 *B* shows the distribution of modulation depths at a saturating Ca^{2+} concentration of 25 μM (Niggli et al., 1981). The low modulation depths demonstrate a highly mobile population of CaM-TMR. However, when the Ca^{2+} concentration is reduced to 0.15 μM, corresponding to roughly one-third of the maximum activation level of PMCA (Niggli et al., 1981), a population having a low mobility appears (Fig. 2 *A*). These experiments thus identify two states of the PMCA-CaM-TMR complex with populations dependent on Ca^{2+} concentration.

Orientational mobility of the fluorophore is possible in a number of degrees of freedom: the fluorophore could reorient with respect to CaM; CaM may reorient with respect to PMCA; and PMCA itself may be reorientationally mobile. As mentioned above, time-resolved fluorescence anisotropy results (see supplemental material) show restricted and incomplete orientational motion of the dye with respect to the protein on the timescale of the fluorescence lifetime. The distribution of modulation depths detected for TMR attached to CaM demonstrates that none of the orientational degrees of freedom results in complete orientational averaging on the timescale of the polarization modulation (40 ms). These results show that TMR does not reorient freely with respect to the protein.

Previous ensemble anisotropy measurements have shown that CaM bound to PMCA in native erythrocyte membranes is orientationally mobile with reorientation on the 80-ns timescale (Yao et al., 1996), significantly faster than the rotational correlation time of PMCA in the membrane (~100 μs) but slower than the rotational time of CaM alone. Since both domains of CaM are tightly associated with binding

sites on the autoinhibitory domain at the Ca^{2+} levels employed, this finding shows that the dissociated autoinhibitory domain is orientationally mobile, with a much higher mobility than PMCA as a whole. Thus, we expected that CaM-TMR molecules would exhibit low modulation for saturating Ca^{2+} concentrations. The distribution in Fig. 2 *B* confirms a high orientational mobility under these conditions. In contrast, the large polarization modulation for some molecules at a reduced Ca^{2+} concentration is striking and reveals that the autoinhibitory domain is orientationally restricted in these cases (see Figs. 1 *C* and 2 *A*). We speculate that this state corresponds to complexes in which CaM is bound to PMCA but the autoinhibitory domain is not dissociated, leaving the pump inactive.

Based on these considerations, we suggest that the single-molecule modulation depth distributions provide a direct means to characterize the populations of PMCA-CaM complexes having dissociated versus nondissociated autoinhibitory domains. The response of the modulation-depth distributions to factors such as Ca^{2+} concentration or ATP that are known to regulate the activity of the pump further supports the interpretation that modulation-depth distributions track the state of the autoinhibitory domain. The modulation-depth distributions thus lead to the conclusion that the fraction of the population of PMCA-CaM complexes with a nondissociated autoinhibitory domain is sensitive to the Ca^{2+} level. At a saturating Ca^{2+} concentration, 10% or fewer of the molecules display a low mobility that can be attributed to a nondissociated autoinhibitory domain (Fig. 2 *B*). At 0.15 μM Ca^{2+}, however, 30% of the molecules belong to a low-mobility population (Fig. 2 *A*), consistent with the reduced activity of PMCA at a reduced Ca^{2+} level.

The distributions of modulation depths in Fig. 2 demonstrate that the standard two-state model of the function of the Ca^{2+} pump cannot be correct. In this model (Enyedi et al., 1989; Falchetto et al., 1991),

$$PMCA_{inhibited} + CaM \leftrightarrow PMCA_{active}\text{-}CaM,$$

the pump is inactive with a nondissociated autoinhibitory domain in the absence of CaM and active with a dissociated autoinhibitory domain when CaM is bound to PMCA. As the Ca^{2+} level is decreased, the activity of PMCA decreases. The fraction of PMCA with bound CaM also decreases, as observed in the decreasing number of single-molecule images from PMCA-CaM complexes. If a two-state model were correct, then the $PMCA_{active}$-CaM complexes still detected would yield a distribution of modulation depths identical to the distribution at higher Ca^{2+} levels. Instead, as the Ca^{2+} concentration is decreased, a population of PMCA-CaM complexes having low mobility appears (Fig. 2 *A*). Thus, another state must be present corresponding to PMCA-CaM complexes having an increased modulation depth, i.e., a decreased orientational mobility, a feature inconsistent with a simple two-state model.

The autoinhibitory domain consists of a cytosolic segment located near the C-terminus of PMCA. The reduced activity at lower Ca^{2+} suggests the hypothesis that the low-mobility state does not provide CaM stimulation of PMCA activity, though CaM is still bound. This feature thus suggests a three-state model of PMCA. The proposed model for activation of PMCA is illustrated in Fig. 4. The state without CaM bound is inactive, with the autoinhibitory domain blocking the active site (Fig. 4, *left panel*). The right panel in Fig. 4 represents PMCA in its active state, with CaM bound and the autoinhibitory domain dissociated. A third state (*middle panel*), shows CaM bound but the autoinhibitory domain not dissociated. Such a state may arise, for example, by binding of only the C-terminal domain of CaM, but it is also possible that both domains of CaM bind to the pump but in a configuration that does not lead to dissociation of the autoinhibitory domain. Known features of the structure of PMCA are consistent with this model, including the nucleotide-binding site and the presence of an autoinhibitory domain that binds CaM (Enyedi et al., 1989; Falchetto et al., 1991).

A distribution between active and inactive states of the pump with CaM bound could provide a mechanism for regulation of enzyme activity. Penniston and co-workers have suggested that CaM can remain bound to an inactive PMCA at a low Ca^{2+} concentration, affording a memory of the previous saturating Ca^{2+} level (Caride et al., 2001). Their kinetic measurements showed a memory of ~50 s, consistent with a static modulation depth for times of tens of seconds or longer in most single-molecule trajectories, as we have observed (see Fig. 1, for example). The existence of inactive PMCA-CaM complexes may serve an important function in the rapid response to subsequent Ca^{2+} signaling events. Sun and Squier pointed out that CaM with the C-terminal domain bound to the pump but the N-terminal domain dissociated would allow an inactive PMCA-CaM complex to respond rapidly to a transient increase in Ca^{2+} concentration because of the presence of CaM already bound to PMCA (Sun and Squier, 2000).

Orientational mobility in the presence of ATP

In the presence of ATP, enzymatic turnover of PMCA can occur. Fig. 3 shows that ATP favors a high-mobility (low modulation depth) state of the PMCA-CaM complex at both

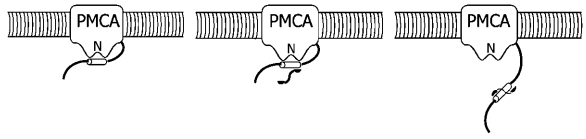

FIGURE 4 Proposed model of the CaM binding and activation of PMCA. The left panel shows PMCA with a bound autoinhibitory domain. The right panel shows PMCA with CaM bound and the autoinhibitory domain dissociated. The center panel proposes a third state in which CaM is bound to PMCA without releasing the autoinhibitory domain. *N* denotes the nucleotide-binding site.

a saturating Ca^{2+} concentration (25 μM) and a reduced Ca^{2+} concentration (0.15 μM). In both cases, the fraction of population present in the low-mobility (high modulation depth) state is lower than in the distributions for PMCA-CaM lacking ATP (Fig. 2). As discussed above, we attribute the population of PMCA-CaM with a high mobility to PMCA-CaM complexes with a dissociated autoinhibitory domain. The modulation-depth distributions in Fig. 3 show that in the cycling pump, PMCA-CaM complexes have a high orientational mobility characteristic of a dissociated autoinhibitory domain, even at the reduced Ca^{2+} concentration of 0.15 μM. This suggests that association of the autoinhibitory domain with its binding sites in the nucleotide and phosphorylation domains occurs in a state of the pump that is inaccessible or kinetically short-lived in the presence of ATP. The loss of the low-mobility population in the presence of ATP further suggests that binding of ATP or subsequent ATP hydrolysis and phosphorylation of the pump disrupts association of the autoinhibitory domain with its binding sites. The structural basis of this coupling is not currently known. It may be that ATP binding or utilization induces changes in the relative conformations of the cytosolic domains of the pump that alter the availability of inhibitory domain binding sites. Such changes in the relative orientations of domains of the homologous (although lacking an autoinhibitory domain) sarcoplasmic-endoplasmic reticulum Ca^{2+}-ATPase (SERCA) have been observed in crystal structures of SERCA (Toyoshima and Nomura, 2002; Xu et al., 2002).

A clue to the basis for association of the autoinhibitory domain binding is offered by the modulation-depth distributions in the presence of the ATP analog, AMP-PNP, which binds to the nucleotide-binding site but is not hydrolyzed. The modulation depth distributions of PMCA with AMP-PNP (Fig. 3) display the presence of a low-mobility population at a reduced Ca^{2+} concentration of 0.15 μM. Thus, the inability of the pump to become phosphorylated permits the formation of a population of reduced orientational mobility as the Ca^{2+} level is reduced. Based on the interpretation offered above, we can conclude that the autoinhibitory domain can associate with the pump in the state with a ligand bound to the nucleotide-binding site, but not after phosphorylation. This picture is consistent with a model proposed by Stokes and co-workers for the function of the SERCA Ca^{2+} pump in which phosphorylation stabilizes a new conformation of the pump (Xu et al., 2002).

CONCLUSIONS

We have demonstrated the ability of single-molecule polarization modulation to detect states of PMCA throughout the catalytic cycle. The results demonstrate the power of single-molecule investigations to reveal features of biomolecular systems that are hidden in ensemble measurements. In regulating intracellular Ca^{2+} levels, CaM reversibly binds and activates PMCA, a transmembrane Ca^{2+} pump, at Ca^{2+} levels of 0.05 μM or higher (Caride et al., 2001). Single-molecule polarization modulation experiments provide a means to map out the orientational mobility of the autoinhibitory domain in single molecules and reveal heterogeneous populations that depend on Ca^{2+} concentration and ATP. PMCA-CaM-TMR complexes are sensitive to Ca^{2+} concentration. At a saturating Ca^{2+} concentration, the modulation depth distribution reveals a mobile population. We can therefore attribute this population to PMCA-CaM complexes with a dissociated autoinhibitory domain. In contrast, we have found a less mobile conformation of the PMCA-CaM complexes at a lower Ca^{2+} concentration.

The Ca^{2+}-dependent binding of CaM is thought to stimulate the release of the autoinhibitory domain from the nucleotide-binding site of PMCA. The single-molecule mobilities measured here support this mechanism of regulation of PMCA. However, they also show that this picture is incomplete, because it does not account for the low-mobility population. We suggest that the low-mobility population can be attributed to a state with CaM-TMR bound but the autoinhibitory domain not dissociated. Such a state would occur at nonsaturating Ca^{2+} concentrations, where the Ca^{2+}-binding sites in the N-terminal domain of CaM are not occupied (Yazawa et al., 1992). Under these conditions, the N-terminal domain of CaM may be dissociated or only loosely bound to PMCA.

In contrast to the distributions in the absence of ATP, the distributions of modulation depths in the presence of ATP are independent of Ca^{2+} concentration. This reveals a response of the autoinhibitory domain to ATP binding or subsequent hydrolysis and phosphorylation of the enzyme such that the autoinhibitory domain remains dissociated even at the reduced Ca^{2+} concentration. The ability of ATP to affect the binding dynamics of the autoinhibitory domain may reflect long-range structural couplings between the nucleotide-binding site and other protein domains. Motions that drive Ca^{2+} transport may change the structural conformations of PMCA so that binding of the autoinhibitory domain is less favorable. Binding of the structurally similar but nonhydrolyzable ATP analog, AMP-PNP, leads to the presence of the low-mobility population of PMCA-CaM complexes at a low Ca^{2+} concentration, suggesting that it is phosphorylation of the enzyme that inhibits association of the autoinhibitory domain.

SUPPLEMENTARY MATERIAL

An online supplement to this article can be found by visiting BJ Online at http://www.biophysj.org.

We are grateful to Jeff Urbauer, Thomas Squier, and Mary L. Michaelis for helpful discussions. We thank Erik Sanchez for the data collection software and Jay Unruh for the fluorescence anisotropy measurement of CaM-TMR. C.K.J. wishes to thank Sunney Xie, Steve Colson, and the Chemical

Structure and Dynamics group at the Environmental Molecular Sciences Laboratory for gracious hospitality and financial support during a sabbatical stay at Pacific Northwest National Laboratory.

This work was supported by National Institutes of Health grants RO1 GM58715 and AG12993, the American Heart Association (99513262), and a Research Corporation Research Opportunity Award.

REFERENCES

Adachi, K., R. Yasuda, H. Noji, H. Itoh, Y. Harada, M. Yoshida, and K. Kinosita, Jr. 2000. Stepping rotation of F1-ATPase visualized through angle-resolved single-fluorophore imaging. *Proc. Natl. Acad. Sci. USA.* 97:7243–7247.

Allen, M. W., R. J. B. Urbauer, A. Zaidi, T. D. Williams, J. L. Urbauer, and C. K. Johnson. 2004. Fluorescence labeling, purification and immobilization of a double cysteine mutant calmodulin fusion protein for single-molecule experiments. *Anal. Biochem.* 325:273–284.

Babu, Y. S., C. E. Bugg, and W. J. Cook. 1988. Structure of calmodulin refined at 2.2 Å resolution. *J. Mol. Biol.* 204:191–204.

Carafoli, E. 1987. Intracellular calcium homeostasis. *Annu. Rev. Biochem.* 56:395–433.

Caride, A. J., N. L. Elwess, A. K. Verma, A. G. Filoteo, A. Enyedi, Z. Bajzer, and J. T. Penniston. 1999. The rate of activation by calmodulin of isoform 4 of the plasma membrane Ca^{2+} pump is slow and is changed by alternative splicing. *J. Biol. Chem.* 274:35227–35232.

Caride, A. J., A. R. Penheiter, A. G. Filoteo, Z. Bajzer, A. Enyedi, and J. T. Penniston. 2001. The plasma membrane calcium pump displays memory of past calcium spikes. Differences between isoforms 2b and 4b. *J. Biol. Chem.* 276:39797–39804.

Crivici, A., and M. Ikura. 1995. Molecular and structural basis of target recognition by calmodulin. *Annu. Rev. Biophys. Biomol. Struct.* 24:85–116.

Enyedi, A., T. Vorherr, P. James, D. J. McCormick, A. G. Filoteo, E. Carafoli, and J. T. Penniston. 1989. The calmodulin binding domain of the plasma membrane Ca^{2+} pump interacts both with calmodulin and with another part of the pump. *J. Biol. Chem.* 264:12313–12321.

Fabiato, A., and F. Fabiato. 1979. *J. Physiol. (Paris).* 75:463–505.

Falchetto, R., T. Vorherr, J. Brunner, and E. Carafoli. 1991. The plasma membrane Ca^{2+} pump contains a site that interacts with its calmodulin-binding domain. *J. Biol. Chem.* 266:2930–2936.

Forkey, J. N., M. E. Quinlan, M. A. Shaw, J. E. Corrie, and Y. E. Goldman. 2003. Three-dimensional structural dynamics of myosin V by single-molecule fluorescence polarization. *Nature.* 422:399–404.

Ha, T., T. A. Laurence, D. S. Chemla, and S. Weiss. 1999. Polarization spectroscopy of single fluorescent molecules. *J. Phys. Chem. B.* 103: 6839–6850.

Harms, G. S., S. W. Pauls, J. F. Hedstrom, and C. K. Johnson. 1997. Tyrosyl fluorescence decays and rotational dynamics in tyrosine monomers and in dipeptides. *J. Fluoresc.* 7:273–282.

Lanzetta, P. A., L. J. Alvarez, P. S. Reinach, and O. A. Candia. 1979. An improved assay for nanomole amounts of inorganic phosphate. *Anal. Biochem.* 100:95–97.

Lu, H. P., L. Xun, and X. S. Xie. 1998. Single-molecule enzymatic dynamics. *Science.* 282:1877–1882.

Moerner, W. E., and M. Orrit. 1999. Illuminating single molecules in condensed matter. *Science.* 283:1670–1676.

Niggli, V., E. S. Adunyah, J. T. Penniston, and E. Carafoli. 1981. Purified (Ca^{2+}-Mg^{2+})-ATPase of the erythrocyte membrane. Reconstitution and effect of calmodulin and phospholipids. *J. Biol. Chem.* 256:395–401.

Noji, H., R. Yasuda, M. Yoshida, and K. Kinosita. 1997. Direct observation of the rotation of F_1-ATPase. *Nature.* 386:299–302.

Osborn, K. D. 2003. Single-Molecule Studies of the Interaction of Calmodulin with the Plasma Membrane Ca^{2+}-ATPase. PhD dissertation. University of Kansas, Lawrence.

Osborn, K. D., M. K. Singh, R. J. B. Urbauer, and C. K. Johnson. 2003. Maximum likelihood approach to single-molecule polarization modulation analysis. *Chem. Phys. Chem.* 4:1005–1011.

Penniston, J. T., and A. Enyedi. 1998. Modulation of the plasma membrane Ca^{2+} pump. *J. Membr. Biol.* 165:101–109.

Peterman, E. J., H. Sosa, L. S. Goldstein, and W. E. Moerner. 2001. Polarized fluorescence microscopy of individual and many kinesin motors bound to axonemal microtubules. *Biophys. J.* 81:2851–2863.

Sosa, H., E. J. Peterman, W. E. Moerner, and L. S. Goldstein. 2001. ADP-induced rocking of the kinesin motor domain revealed by single-molecule fluorescence polarization microscopy. *Nat. Struct. Biol.* 8: 540–544.

Stauffer, T. P., D. Guerini, and E. Carafoli. 1995. Tissue distribution of the four gene products of the plasma membrane Ca^{2+} pump. *J. Biol. Chem.* 270:12184–12190.

Sun, H., and T. C. Squier. 2000. Ordered and cooperative binding of opposing globular domains of calmodulin to the plasma membrane Ca-ATPase. *J. Biol. Chem.* 275:1731–1738.

Toyoshima, C., and H. Nomura. 2002. Structural changes in the calcium pump accompanying the dissociation of calcium. *Nature.* 418:605–611.

Van Eldik, L. J., and D. M. Watterson. 1998. Calmodulin and Signal Transduction. Academic Press, New York.

Vogel, H. J. 1994. Calmodulin: a versatile calcium mediator protein. *Biochem. Cell Biol.* 72:357–376.

Warshaw, D. M., E. Hayes, D. Gaffney, A. M. Lauzon, J. Wu, G. Kennedy, K. Trybus, S. Lowey, and C. Berger. 1998. Myosin conformational states determined by single fluorophore polarization. *Proc. Natl. Acad. Sci. USA.* 95:8034–8039.

Weiss, S. 1999. Fluorescence spectroscopy of single biomolecules. *Science.* 283:1676–1683.

Xie, X. S., and R. C. Dunn. 1994. Probing single molecule dynamics. *Science.* 265:361–364.

Xie, X. S., and H. P. Lu. 1999. Single-molecule enzymology. *J. Biol. Chem.* 274:15967–15970.

Xie, X. S., and J. K. Trautman. 1998. Optical studies of single molecules at room temperature. *Annu. Rev. Phys. Chem.* 49:441–480.

Xu, C., W. J. Rice, W. He, and D. L. Stokes. 2002. A structural model for the catalytic cycle of Ca^{2+}-ATPase. *J. Mol. Biol.* 316:201–211.

Yao, Y., J. Gao, and T. C. Squier. 1996. Dynamic Structure of the calmodulin-binding domain of the plasma membrane Ca-ATPase in native erythrocyte ghost membranes. *Biochemistry.* 35:12015–12028.

Yazawa, M., T. Vorherr, P. James, E. Carafoli, and K. Yagi. 1992. Binding of calcium by calmodulin: influence of the calmodulin binding domain of the plasma membrane calcium pump. *Biochemistry.* 31:3171–3176.